Title:
Cylinder-based Simultaneous Registration and Model Fitting of Laser-scanned Point Clouds for Accurate As-built Modeling of Plant Piping Systems

Authors:
Ryota Moritani, r_moritani@sdm.ssi.ist.hokudai.ac.jp, Hokkaido University
Satoshi Kanai, kanai@ssi.ist.hokudai.ac.jp, Hokkaido University
Hiroaki Date, hdate@ssi.ist.hokudai.ac.jp, Hokkaido University
Masahiro Watanabe, masahiro.watanabe.ub@hitachi.com, Hitachi, Ltd.
Takahiro Nakano, takahiro.nakano.tz@hitachi.com, Hitachi, Ltd.
Yuta Yamauchi, yuta.yamauchi.kj@hitachi.com, Hitachi, Ltd.

Keywords:
Laser Scanning, Registration, Point Clouds, Piping System, Terrestrial laser scanner

DOI: 10.14733/cadconfP.2017.389-394

Introduction:

Three-dimensional laser scanning and as-built CAD modeling of complex piping systems are increasingly used in plant engineering. In as-built modeling, multiple partially scanned point clouds of objects largely composed of cylindrical pipes are captured from different viewpoints by a terrestrial laser scanner (TLS). The registration process aligns these point clouds into a consistent coordinate system. The pipe parameters are then estimated by fitting cylinders to the registered point clouds. Therefore, both the registration and cylinder model fitting must be sufficiently accurate for as-built modeling of piping systems.

As shown Fig. 1., we propose a new algorithm for registration and model fitting of laser-scanned point clouds. The algorithm is specialized for as-built modeling of the cylindrical pipes of plants. Unlike the ICP-based method, our model simultaneously solves the fine registration and model fitting problem by expressing them as a single nonlinear constraint equation. This fine registration works even when the overlap between scans is completely absent, and achieves a more accurate registration and fitting than the ICP-based method. The coarse registration is automated by assigning the cylindrical surfaces in the scans as geometric features for the alignment. This paper describes the proposed algorithm and compares its accuracy with that of a conventional ICP-based method in scan simulations.

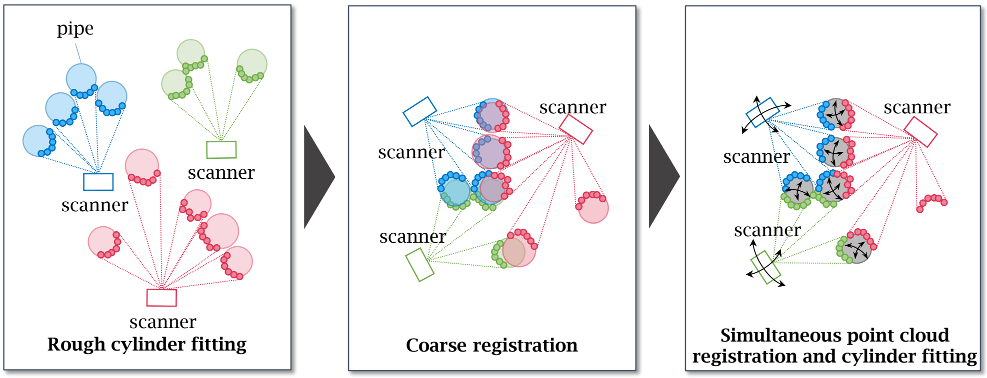

Fig. 1: Registration and model fitting of scanned points of piping systems.

Related Work:

Point cloud registration is an indispensable processing for aligning multiple partial scans captured from different scanner positions into a consistent coordinate. Maker-less methods are subdivided into the ones for fine and coarse registrations. The most well-known fine registration algorithm is the Iterative Closest Point (ICP) [2], where the sum of squared distance between closest points in two scans are minimized to obtain the best transformation which aligns them. Unlike the ICP, fine registration methods minimizing the sum of squares of the distance between the surfaces in the point clouds are proposed [6], and any kind of 3D surface correspondence problem can be solved in these methods. However, a problem of these minimization-based fine-registration methods is that enough overlaps between two scans and good initial alignment between two scans are essential for achieving a convergence to a precise alignment. If the overlap between scans is small or absent or the initial alignment includes some amount of deviation, the registration result converges to an incorrect solution.

On the other hand, many maker-less coarse registration methods for TLS point clouds have also been intensively studied to estimate consistent initial alignment between different scans for fine registration [9]. These methods extract variety of available geometric features from the scans and estimate the initial alignments with small deviations. A variety of the geometric features have been used for the registration such as point, line and plane features. Examples of point features include SIFT feature points in TLS reflectance images [11]. Line features [1] and plane features [7] are also proposed. However, these methods only aim for the coarse alignment and cannot necessarily achieve the registration accuracy required for the accurate model fitting of the piping systems. Moreover, although cylinders constitute a vast majority of the surfaces in the scanned point clouds of piping systems, the cylindrical features have not been efficiently used in these coarse registrations.

Cylinder-based Coarse Scan Registration using RANSAC:

The coarse scan registration is performed by a RANSAC-based algorithm, and proceeds through the following steps. 1) In the j-th scan s^j, a set of radii and axes of cylindrical surfaces $\{(r_k^j, \boldsymbol{a}_k^j)\}$ is extracted from the point clouds using PCA-based normal estimation and MSAC-based [10] or efficient-RANSAC-based [8] cylinder fitting. 2) A hash table is constructed whose key value corresponds to the distance $dist(\boldsymbol{a}_n^0, \boldsymbol{a}_m^0)$ between every pair of non-parallel cylinder axes $(\boldsymbol{a}_n^0, \boldsymbol{a}_m^0)$ in the target scan s^0. 3) A pair of non-parallel cylinder axes $(\boldsymbol{a}_{n'}^j, \boldsymbol{a}_{m'}^j)$ is randomly picked up from a source scan s^j, and the pair of axes $(\boldsymbol{a}_n^0, \boldsymbol{a}_m^0)$ with closest distance to $dist(\boldsymbol{a}_{n'}^j, \boldsymbol{a}_{m'}^j)$ is retrieved in the hash table. 4) A transformation aligns the non-parallel cylinder axes $(\boldsymbol{a}_{n'}^j, \boldsymbol{a}_{m'}^j)$ in s^j with $(\boldsymbol{a}_n^0, \boldsymbol{a}_m^0)$ in s^0, and the degree of coincidence between the other corresponding axes in s^j and s^0 is evaluated. 5) Steps 3) and 4) are iterated until the transformation giving the best coincidence is applied to the source scan s^j. 6) The union of scans $s^0 \cup s^j$ becomes the new target scan, and steps 3) to 5) are repeated for the other source scan $s^{j'}$.

Cylinder-based Fine Scan Registration Based on Simultaneous Alignment and Model Fitting:

Basic concept of fine scan registration

The proposed fine scan registration minimizes the sum of the fitting error at each point scanned from the corresponding exact cylindrical surface. As shown in Fig. 2., The minimization simultaneously adjusts the registration parameters (positions and orientations) of the scanners and the model parameters (positions, orientations and radii) of the cylinders. The minimization is formulated as follows:

$$\min_{\{\boldsymbol{x}_j^{Reg}\}\{\boldsymbol{x}_k^{Cyl}\}} \sum_{j\in B-\{t_0\}} \sum_{k\in C} \sum_{i\in P_k} \left[D_{jk}\left(i\,;\,\boldsymbol{x}_j^{Reg},\ \boldsymbol{x}_k^{Cyl}\right)\right]^2 \tag{1}$$

where, B is a set of scanners, t_0 is a scanner at a reference (fixed) location, and C is a set of uniquely identified cylinders in all scans $\{s^j\}$. P_k denotes a set of scanned points placed on cylinder k, and $\boldsymbol{x}_k^{Cyl}$ are the model parameters of cylinder k. $\boldsymbol{x}_j^{Reg}$ denotes the registration parameters of scanner j. $D_{jk}(i;\ \boldsymbol{x}_j^{Reg}, \boldsymbol{x}_k^{Cyl})$ denotes the fitting error function of a scanned point i from cylinder k located at $\boldsymbol{x}_k^{Cyl}$, when point i is captured by scanner j located at $\boldsymbol{x}_j^{Reg}$. This simultaneous adjustment of $\boldsymbol{x}_j^{Reg}$ and $\boldsymbol{x}_k^{Cyl}$ prevents the alignment error of the fine registration from propagating through the following model fitting, and helps preserve the modeling accuracy of the piping system. This research alternates two fitting error functions

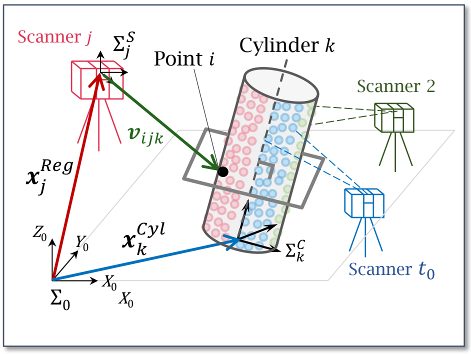

Fig. 2: Fine scan registration.

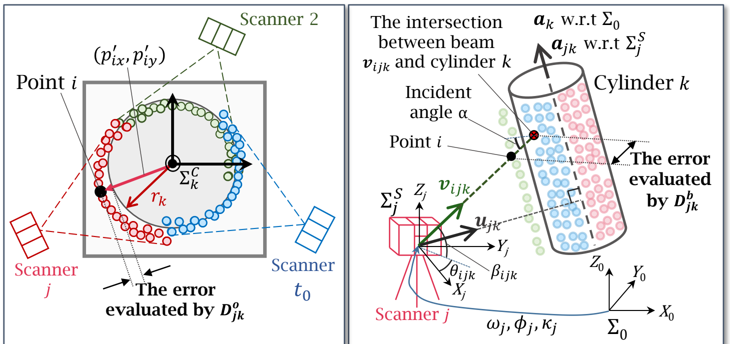

(a) Orthogonal error function D_{jk}^o (b) Beam direction error function D_{jk}^b

Fig. 3: (a) Orthogonal error function and (b) beam direction error function.

D_{jk}; the *orthogonal direction error* D_{jk}^o and the *beam direction error* D_{jk}^b. The modeling accuracy depends on the function type, as discussed in a later section.

Precise Cylinder Alignment by minimizing Errors along an Orthogonal Direction

The orthogonal error function D_{jk}^o evaluates the squared orthogonal distance of a point from its corresponding cylindrical surface. To simplify the evaluation, we first classify the direction of a cylinder axis obtained from the course registration into one of the three dominant orthogonal axial directions (X_0, Y_0 or Z_0) in a world coordinate system Σ_0, as proposed in [3]. For example, as shown in Fig. 3(a)., when a cylinder axis is nearly parallel to the Z_0 axis, the error function D_{jk}^o is defined by Eqs. (2) and (3):

$$D_{jk}^o\left(i\,;\,\boldsymbol{x}_j^{Reg}, \boldsymbol{x}_k^{Cyl}\right) = p_{ix}'^2 + p_{iy}'^2 - r_k^2 \tag{2}$$

$$\boldsymbol{p}_i' = \mathrm{R}(\Phi_k)\mathrm{R}(\Omega_k)\,\{\boldsymbol{p}_i - \boldsymbol{q}_k\} \tag{3}$$

where $\boldsymbol{p}_i = \left[\,p_{ix}, p_{iy}, p_{iz}\,\right]^t$ and $\boldsymbol{p}_i' = \left[p_{ix}', p_{iy}', p_{iz}'\,\right]^t$ are the positions of a point i w.r.t. Σ_0 and a local coordinate system Σ_k^C fixed on cylinder k, with radius $r_k (\in \boldsymbol{x}_k^{Cyl})$, respectively. $\boldsymbol{q}_k = \left[\,q_{kx}, q_{ky},\ 0\,\right]^t (\in \boldsymbol{x}_k^{Cyl})$ is the intersection point between the cylinder axis and the X_0Y_0 plane w.r.t. Σ_0, R( ) is a 3 × 3 rotation matrix, and $\Omega_k (\in \boldsymbol{x}_k^{Cyl})$ and $\Phi_k (\in \boldsymbol{x}_k^{Cyl})$ are the rotational angles about the X_0 and Y_0 axis, respectively. These angles specify the axial orientation of cylinder k. Cylinder axes nearly parallel to the X_0 or Y_0 axis are formulated similarly.

Precise Cylinder Alignment by minimizing Errors along the Beam Direction

The accidental error of the scan follows a normal distribution along the beam incident direction at a scanned point. Therefore, as shown in Fig. 3(b), the beam direction error function D_{jk}^b evaluates the distance of point i from its corresponding cylindrical surface k along the laser beam direction emitted by the scanner, as described by Eqs. (4), (5), and (6).

$$D_{jk}^b\left(i\,;\,\boldsymbol{x}_j^{Reg}, \boldsymbol{x}_k^{Cyl}\right) = \left(\lambda - \sqrt{\lambda^2 - \kappa\mu}\right)/\kappa - d_i \tag{4}$$

$$\kappa = 1 - \left(\boldsymbol{a}_{jk} \cdot \boldsymbol{v}_{ijk}\right)^2,\ \ \lambda = \rho_{jk}\left(\boldsymbol{v}_{ijk} \cdot \boldsymbol{n}_{jk}\right),\ \ \mu = \rho_{jk}^2 - r_k^2 \tag{5}$$

$$\boldsymbol{a}_{jk} = \mathrm{R}(\kappa_j)\mathrm{R}(\phi_j)\mathrm{R}(\omega_j)\boldsymbol{a}_k, \quad \boldsymbol{n}_{jk} = \boldsymbol{u}_{jk}'/\rho_{jk}, \quad \rho_{jk} = \left\|\boldsymbol{u}_{jk}'\right\|, \quad \boldsymbol{u}_{jk}' = \mathrm{R}(\kappa_j)\mathrm{R}(\phi_j)\mathrm{R}(\omega_j)\boldsymbol{u}_{jk} \tag{6}$$

Here, $\boldsymbol{a}_k$ and $\boldsymbol{a}_{jk}$ are the unit axis vectors of cylinder k w.r.t. Σ_0 and the local coordinate system Σ_j^S fixed at scanner j, respectively. The angles $\omega_j, \phi_j, \kappa_j (\in \boldsymbol{x}_j^{Reg})$ specify the orientations of the X_j, Y_j and Z_j axes of Σ_j^S w.r.t. Σ_0. $\boldsymbol{v}_{ijk} = \left[\cos\beta_{ijk}\cos\theta_{ijk}\,, \cos\beta_{ijk}\sin\theta_{ijk}\,,\ \sin\beta_{ijk}\right]^t$ is the unit vector of the beam emitted by scanner j incident at point i on cylinder k, where θ_{ijk} and β_{ijk} denote the azimuthal and elevation angles, respectively, of the beam from scanner j w.r.t. Σ_j^S. $\boldsymbol{u}_{jk} = \left[u_{jkx}, u_{jky}, u_{jkz}\right]^t$ is a point position on the axis of the cylinder k closest to the origin of Σ_j^S w.r.t. Σ_0.

Optimization Process

Adopting the error function D_{jk}^{o} of Eqs. (2) and (3) or the D_{jk}^{b} of Eqs. (4), (5) and (6) as D_{jk}, the minimization problem Eq. (1) is solved for the registration parameters $\{\boldsymbol{x}_j^{Reg}\}$ and model parameters $\{\boldsymbol{x}_k^{Cyl}\}$. Each error function D_{jk} represents a fitting error of a cylinder, which ideally converges to zero. Plausible initial guesses of the parameters $\boldsymbol{x}_j^{Reg}$ and $\boldsymbol{x}_k^{Cyl}$ are known from the coarse registration. Therefore, to find the solutions $\{\boldsymbol{x}_j^{Reg}\}$ and $\{\boldsymbol{x}_k^{Cyl}\}$ of Eq. (1), we simply solve a large set of simultaneous nonlinear equations of the form $D_{jk}(i;\ \boldsymbol{x}_j^{Reg}, \boldsymbol{x}_k^{Cyl}) = 0$ by Newton's method.

The parameters are fine-tuned by one of two methods. The first method filters out the set of scanned points from P_k in Eq. (1) whose beam incident angle exceeds the threshold α_{th}. This method eliminates the large rise in accidental error at incident angles above 60°. The second method assumes that the radius r_k is chosen from standardized discrete pipe radii. Once the optimum solutions are found, an additional convergence step is implemented on variables $\{\boldsymbol{x}_k^{Cyl}\} - \{r_k\}$.

<u>Modeling and Registration Accuracies:</u>

To precisely evaluate the accuracy of model fitting and registration, a scan simulation software was developed. This software generates laser-scanned point clouds in the 3D CAD model of a piping system and superimposes artificial measurement errors on the point clouds. The errors are generated according to the model $\varepsilon(d,\alpha) \sim \aleph(\mu(d,\alpha), \sigma^2(d,\alpha))$, where $\aleph(\mu,\sigma^2)$ denotes a normal distribution and the average μ and standard deviation σ uniquely depend on the scan distance d and the beam incident angle α.

	Without incident angle filtering	With incident angle filtering
Orthogonal direction error	**Condition I** (Solution converged)	**Condition II** (Solution converged)
Beam direction error	(Solution is not converged)	**Condition III** (Solution converged)
Built-in ICP-based registration in commercial software	**Condition IV** (Cloud-Compare) **Condition V** (Geomagic) (Solution converged)	—

Tab. 1: Fine registration conditions and convergence status of the solution.

Using the scan simulation software, the scanned point clouds with 19 million error points captured from three scanner positions are generated by the CAD model of a piping system (10 m × 15 m × 9 m) (see Fig. 4(a).). The point clouds are processed first by the proposed coarse registration (Fig. 4(b).), then by the fine registration, which includes manually-selected six cylinders. To compare the accuracies, the fine registration was executed under four conditions (see Tab 1.). Conditions I, II, and III in the proposed fine registration differ by their error function types and incident angle filtering. Under conditions IV and V, the fine registration is executed by built-in ICP-based registration functions in the free software Cloud-Compare [4] and by the commercial software Geomagic-Wrap [5], respectively. The cylinders were then individually fitted to the aligned point clouds by the Levenberg–Marquardt method. Panels (c) and (d) of Fig. 4. show the fine registration results under conditions II and IV, respectively.

Fig. 5. shows the distributions of the distance error E_d, angle error E_a and cylinder radius error E_r between two cylinders axes. Because we can refer to the original CAD model, the errors are evaluated by comparison with the exact values. As confirmed in Fig. 5., the accuracy of the proposed fine registration method was higher under condition II (orthogonal error with incident angle filtering) than under the other conditions. Conversely, when adopting the beam direction error with incident angle filtering, the minimization of Eq. (1) sometimes failed, causing problems in the registration.

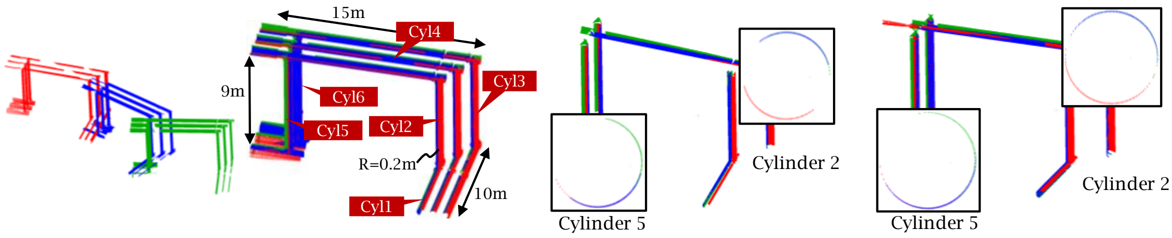

(a) Scanned point clouds before registration

(b) Point clouds after the coarse registration

(c) Point clouds after the fine registration under condition II

(d) Point clouds after the fine registration under condition IV

Fig. 4: Results of coarse and fine registration under conditions II and IV.

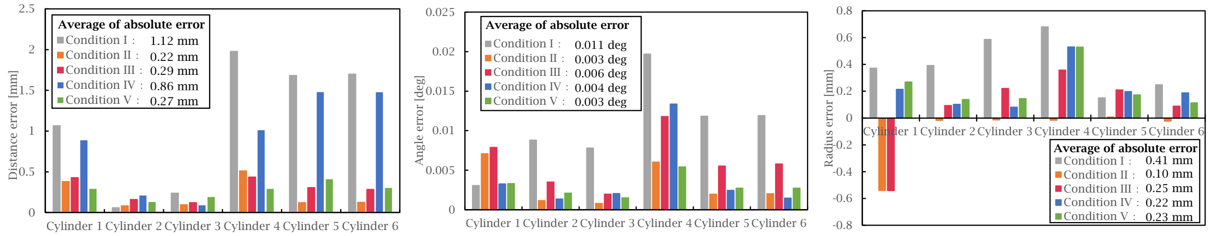

(a) Distance error between two cylinder axes ($\boldsymbol{E_d}$)

(b) Angle error between two cylinder axes ($\boldsymbol{E_a}$)

(c) Radius error of each cylinder ($\boldsymbol{E_r}$)

Fig. 5: Error distributions after fine registration under conditions I to V.

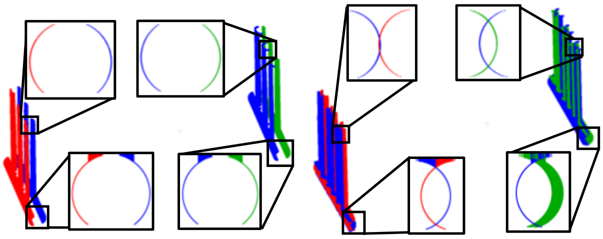

(a) Fine registration result under condition II

(b) Fine registration result under condition IV

Fig. 6: Fine registration results of non-overlapped point clouds.

[mm]

Pipe		Coarse registration	Fine registration
P1	Average	-0.79	-0.01
	Std. dev.	3.51	2.44
P2	Average	-1.51	-0.72
	Std. dev.	7.67	4.37
P3	Average	0.86	-0.04
	Std. dev.	3.50	1.21
P4	Average	10.17	-0.01
	Std. dev.	6.45	1.44

Tab. 2: Distributions of the radius errors at four sampled pipes (P1~P4) in coarse and fine registration

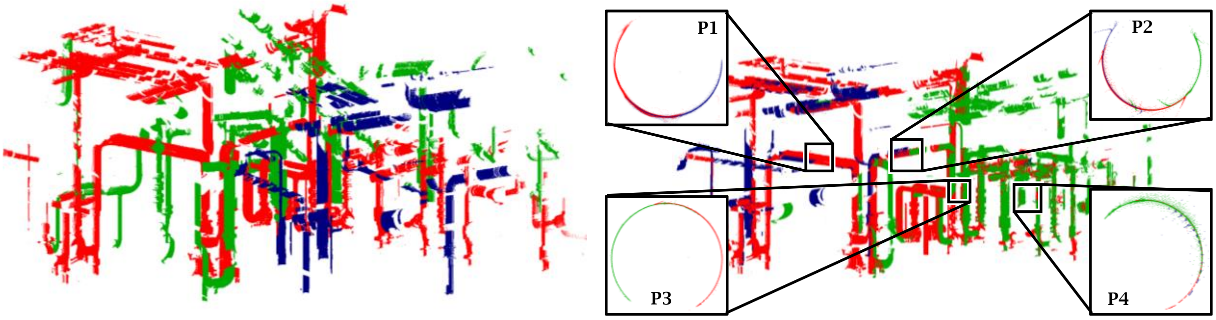

(a) Scanned point clouds before registration

(b) Fine registration result under condition I

Fig. 7: Results of coarse and fine registration for an HVAC plant under conditions I.

Next, the proposed fine registration under conditions I, II, IV, and V were applied to a critical case of no overlap between two scanned point clouds of the pipes. As shown in Fig. 6., both of the proposed fine registrations (conditions I and II) succeeded with acceptable errors (Fig. 6(a).), whereas those of the free and commercial software failed (Fig. 6(b).).

Finally, the proposed modeling and registration method under condition I was applied to actual scanned point clouds captured from the piping system (20m × 15m × 8m) of an urban HVAC plant by a terrestrial laser scanner (Leica, HDS7000). As shown Fig. 7(a)., these clouds contained 1.4 million points after background point clouds except for pipes were manually removed in advance. Fig. 7(b). shows the aligned point clouds after the fine registration under conditon I. Tab. 2 shows how the deviation among three scans and the distribution of the radius errors at four sampled pipes decreased after the proposed fine registration. The result showed that the average errors decreased to sub-millimeter level in all sampled pipes, and their standard deviations also reduced despite a good number of outlier points near the surface shown in Fig. 7(b). This result confirmed that the proposed modeling and registration method could work well for actual laser-scanned point clouds. The fine registration time took 1 min.

Conclusions:

We proposed an algorithm for registration and model fitting of laser-scanned point clouds. The algorithm is specialized for as-built modeling of the cylindrical pipes of plants. An automated coarse registration method was realized through RANSAC. Unlike the conventional ICP-based method, the proposed fine registration and cylinder model fitting are simultaneously performed by solving a nonlinear equation. In simulation studies, the proposed algorithm outperformed the conventional ICP-based registration in both accuracy and robustness to zero scan overlap. The effectiveness for the real scanned data was also proved.

References:

[1] Al-Durgham, K.; Habib, A.; Kwak, E.: RANSAC approach for automated registration of terrestrial laser scans using linear features, ISPRS Ann. Photogramm. Remote Sens. Spatial Inf. Sci., II-5/W2, 2013, 13-18. http://dx.doi.org/10.5194/isprsannals-II-5-W2-13-2013

[2] Besl, P.J.; McKay, N.D.: A method for registration of 3-D shapes, IEEE Trans. on Pattern Analysis and Machine Intelligence, 14(2), 1992, 239-256. http://dx.doi.org/10.1109/34.121791

[3] Chan, T.O.; Lichti, D.D.; Belton, D.: A rigorous cylinder-based self-calibration approach for terrestrial laser scanners, ISPRS Journal of Photogrammetry and Remote Sensing, 99, 2015, 84-99. http://dx.doi.org/10.1016/j.isprsjprs.2014.11.003

[4] Cloud-Compare, http://www.danielgm.net/cc/.

[5] Geomagic-Wrap, http://www.geomagic.com/en/products/wrap/overview, 3D systems.

[6] Ge, X.; Wunderlich, T.: Surface-based matching of 3D point clouds with variable coordinates in source and target system, ISPRS Journal of Photogrammetry and Remote Sensing, 111(1), 2016, 1-12. http://dx.doi.org/10.1016/j.isprsjprs.2015.11.001

[7] Previtali, M.; Barazzetti, L.; Brumana, R.; Scaioni, M.: Laser scan registration using planar features, Int. Arch. Photogramm. Remote Sens. Spatial Inf. Sci., XL-5, 2014, 501-508. http://doi.org/10.5194/isprsarchives-XL-5-501-2014

[8] Schnabel, R.; Wahl, R.; Klein, R.: Efficient RANSAC for point-cloud shape detection, Computer Graphics Forum, 26(2), 2007,1467-8659. http://dx.doi.org/10.1111/j.1467-8659.2007.01016.x

[9] Tam, G.K.L. et al.: Registration of 3D point clouds and meshes: A survey from rigid to nonrigid, IEEE Trans. on Visualization and Computer Graphics, 19(7), 2013, 1199-1217. http://dx.doi.org/10.1109/TVCG.2012.310

[10] Torr, P.H.S.; Zisserman, A.: MLESAC: A new robust estimator with application to estimating image geometry, Computer Vision and Image Understanding, 78(1), 2000, 138-156. http://dx.doi.org/10.1006/cviu.1999.0832

[11] Weinmann, M.; Jutzi, B.: Geometric point quality assessment for the automated, markerless and robust registration of unordered TLS point clouds, ISPRS Ann. Photogramm. Remote Sens. Spatial Inf. Sci., II-3/W5, 2015, 89-96. http://dx.doi.org/10.5194/isprsannals-II-3-W5-89-2015